International Journal of Engineering

Journal Homepage: www.ije.ir

Virtual Flux Based Direct Power Control on Vienna Rectifier

M. Rasouli Khatir, H. Ghoreishy*, S. A. Gholamian

Electrical and Computer Engineering, Babol Noushirvany University of Technology, Babol, Iran

P A P E R I N F O

Paper history:
Received 13 October 2017
Received in revised form 10 November 2017
Accepted 02 December 2017

Keywords:
Capacitor Voltage Balancing
Direct Power Control
Vienna Rectifier
Virtual Flux

A B S T R A C T

This paper proposes the virtual flux based direct power control for Vienna rectifier. No need for the input voltage sensors, the current regulation loop and PWM voltage modulation block along with the active and reactive power decoupling are some of the salient advantages of this method that make it suitable for controlling the conventional active rectifiers. However, due to the three-level nature of the Vienna configuration, balancing the output capacitors voltages is inevitable leading to a modified virtual flux based technique. Applying this modification, a separate switching table has been jammed into the proposed technique in order to control the capacitors voltages. Simulation results show the superiority of the virtual flux technique over the conventional Vienna control techniques from point of the mentioned advantages.

***doi**: 10.5829/ije.2018.31.02b.12*

1. INTRODUCTION

Active rectifiers have gained popularity in recent years. This is due to the increasing use of ac to dc converters and also some major drawbacks of their passive counterparts [1, 2]. Vienna rectifier is a promising active ac to dc converter due to its reduced switch count and lower voltage stress which in turn lead to a reduced switching loss. A three-phase three-level configuration of a Vienna rectifier has been shown in Figure 1. It also has the ability of boosting the input voltage and making the power factor near unity [3-5]. Different conventional control strategies including the carrier-based PWM (continuous and discontinuous), space vector PWM and hysteresis current control have been used to control this converter.

A three-phase Vienna rectifier in reference [6] controls the input current using the hysteresis band control technique. Applying this method reduces the total harmonic distortion (THD) and increases the power factor. However, variable switching frequency and higher switching loss are the disadvantages of the proposed control method.

A discontinuous space-vector modulation for three-level PWM Rectifiers has been proposed by Dalessandro et al. [7]. This technique is just applicable in a limited range of the modulation index. Moreover, strong and expensive microcontrollers are needed to realize the proposed technique.

L. He et al. proposed a carrier-based discontinuous pulse width modulation (CB-DPWM) method [8]. This method is simple compared to the discontinuous PWM method based on space vectors and guarantees normal rectifier operation for all modulation index (m_a) values. Considering the important requirement (IR) factor, an offset voltage will be calculated and then added to the sinusoidal reference. Current values are not presented in offset calculation so this method is not as sensitive as methods which use current values.

The neutral point potential balance is of considerable importance in designing the Vienna converter. Its imbalances increase the equipment voltage stress and also the system harmonics contents [9, 10]. A balanced-factor-calculation based method has been proposed by He and Chen [11] overcoming the problem by setting up neutral point potential model and analyzing the detailed reasons of neutral point imbalance.

This paper proposes the virtual flux based direct power control (VF-DPC) for Vienna rectifier. VF-DPC method has some salient advantages which make it suitable for controlling the conventional active rectifiers.

*Corresponding Author's Email: *ghoreishy@nit.ac.ir* (H. Ghoreishy)

Please cite this article as: M. Rasouli Khatir, H. Ghoreishy, S. A. Gholamian, Virtual Flux Based Direct Power Control on Vienna Rectifier, International Journal of Engineering (IJE), IJE TRANSACTIONS B: Applications Vol. 31, No. 2, (February 2018) 284-291

In DPC, there are no internal current control loops and no PWM modulator block, because the converter switching states are appropriately selected by a switching table based on the instantaneous errors between the commanded and estimated values of active and reactive power. On the other hand, the use of the virtual flux signal for power estimation leads to lower sampling frequency, a simpler voltage and power estimation algorithm and a better dynamic [12].
The Vienna rectifier modeling has been described in section 2. Section 3 states the virtual flux based direct power control for Vienna rectifier which includes the proposed switching table for capacitor voltage balancing. Simulation results will then be carried out in section 4.

2. VIENNA RECTIFIER MODELLING

Figure 1 shows the Vienna rectifier topology which is a combination of a boost converter and a three-phase diode bridge. R_1, R_2, R_3 and L_1, L_2, L_3 are the input three phase resistors and inductors respectively. C_1 and C_2 are the output DC link capacitors. Equations (1) to (3) show the rectifier voltages and currents relationships [7]:

$$\begin{bmatrix} U_{an} \\ U_{bn} \\ U_{cn} \end{bmatrix} = R\begin{bmatrix} I_a \\ I_b \\ I_c \end{bmatrix} + L\begin{bmatrix} \frac{dI_a}{dt} \\ \frac{dI_b}{dt} \\ \frac{dI_c}{dt} \end{bmatrix} + \begin{bmatrix} V_{an} \\ V_{bn} \\ V_{cn} \end{bmatrix} \quad (1)$$

$$I_{c1} = C_1\frac{dV_1}{dt} = \sum_{k=a,b,c}(1-S_k).(\frac{1+SGN(I_k)}{2}).I_k - I_o \quad (2)$$

$$I_{c2} = C_2\frac{dV_2}{dt} = -(\sum_{k=a,b,c}(1-S_k).(\frac{1-SGN(I_k)}{2}).I_k + I_o) \quad (3)$$

where $U_{kn\ (k = a, b, c),}$ is the input three-phase voltage, I_{abc} is the input three-phase line current, $V_{kn\ (k = a, b, c)}$ is the converter three phase voltage and $V_{i\ (i = 1, 2)}$ is the capacitor voltage. $S_{k\ (k = a,b,c)}$ represents the state of switches (1 for the on-state and 0 for the off-state) and $SGN\ (I_{k\ (k = a,b,c)})$ is the current sign of each phase (1 for possitive current sign and 0 for negative current sign). The capacitors voltages are assumed balanced and equal to $V_{dc}/2$.

Based on S_k and $SGN\ (I_k)$, four different equivalent circuits (Figure 2) are formed which determine V_{km}.

Considering phase a, when $SGN\ (I_k) = 1$ and $S_k = 1$, point "a" is connected to the neutral point "m" and $V_{am} = 0$ (Figure 2(a)).

Figure 2(b) shows the Vienna equivalent circuit with the same current sign but $S_k = 0$. So point "a" is connected to the positive polarity of C_1 and $V_{am} = V_{dc}/2$.

On the other hand, when $SGN\ (I_k) = 0$ and $S_k = 1$, point "a" is connected to the neutral point "m" and $V_{am} = 0$ (Figure 2(c)) and in the case of $SGN\ (I_k) = 0$ and $S_k = 0$, point "a" is connected to the negative polarity of C_2 and $V_{am} = -V_{dc}/2$ which is depicted in Figure 2(d).
Equation(4) shows this relationship:

$$V_{km} = (1-S_k).\mathrm{SGN}(\mathrm{I_k}).\frac{V_{DC}}{2}\ ,k=a,\ b\ ,c \quad (4)$$

According to Figure 1, the three phase input voltage can be described as:

$$\begin{bmatrix} V_{an} \\ V_{bn} \\ V_{cn} \end{bmatrix} = \begin{bmatrix} V_{am} \\ V_{bm} \\ V_{cm} \end{bmatrix} + \begin{bmatrix} V_{mn} \\ V_{mn} \\ V_{mn} \end{bmatrix} \quad (5)$$

Assuming that the input voltages and currents are sinusoidal and balanced, the neutral point voltage can be calculated as follows:

$$V_{mn} = -\frac{V_{am}+V_{bm}+V_{cm}}{3} \quad (6)$$

Replacing (6) into (5) yields:

$$\begin{bmatrix} V_{an} \\ V_{bn} \\ V_{cn} \end{bmatrix} = \begin{bmatrix} \frac{2}{3} & -\frac{1}{3} & -\frac{1}{3} \\ -\frac{1}{3} & \frac{2}{3} & -\frac{1}{3} \\ -\frac{1}{3} & -\frac{1}{3} & \frac{2}{3} \end{bmatrix}\begin{bmatrix} V_{am} \\ V_{bm} \\ V_{cm} \end{bmatrix} \quad (7)$$

3. VF-DPC FOR VIENNA RECTIFIER

3. 1. Concept of Virtual Flux for Vienna Rectifier

In the virtual flux based methods, the grid voltage is considered as a three-phase AC motor and the input line resistances and inductances are assumed to be its resistances and inductances, respectively. The virtual flux ($\phi_{\alpha\beta}$) of this motor can be determined by integration of its voltage in the stationary ($\alpha\beta$) reference frame [12]:

$$\phi_{\alpha\beta} = \int U_{\alpha\beta}dt \quad (8)$$

Using Equation (9), the converter voltage in the stationary ($\alpha\beta$) reference frame is expressed by Equations (10) and (11).

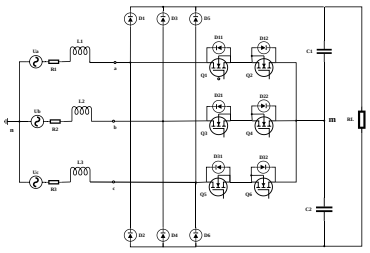

Figure 1. The Vienna rectifier topology

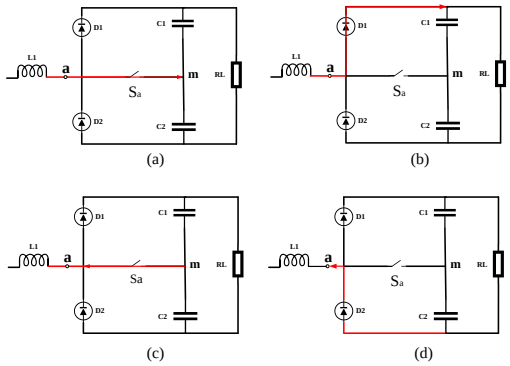

Figure 2. Four different equivalent circuits of the Vienna rectifier. a) *SGN* $(I_k) = 1$ and $S_k = 1$, b) *SGN* $(I_k) = 1$ and $S_k = 0$, c) *SGN* $(I_k) = 0$ and $S_k = 1$ d) *SGN* $(I_k) = 0$ and $S_k = 0$.

$$T = \frac{2}{3}\begin{bmatrix} 1 & -\frac{1}{2} & -\frac{1}{2} \\ 0 & \frac{\sqrt{3}}{2} & -\frac{\sqrt{3}}{2} \end{bmatrix} \tag{9}$$

$$V_\alpha = \frac{2}{3}(\overline{S_a}SGN(I_a) - \frac{1}{2}(\overline{S_a}SGN(I_b) + \overline{S_a}SGN(I_c)))\frac{V_{DC}}{2} \tag{10}$$

$$V_\beta = \frac{1}{\sqrt{3}}(\overline{S_b}SGN(I_b) - \overline{S_c}SGN(I_c))\frac{V_{DC}}{2} \tag{11}$$

Assuming that the input current is sinusoidal and balanced, *Ic* can be rewritten as follows:

$$I_a + I_b + I_c = 0 \rightarrow I_c = -I_a - I_b \tag{12}$$

$$\begin{bmatrix} I_\alpha \\ I_\beta \end{bmatrix} = \frac{2}{3}\begin{bmatrix} 1 & -\frac{1}{2} & -\frac{1}{2} \\ 0 & \frac{\sqrt{3}}{2} & -\frac{\sqrt{3}}{2} \end{bmatrix}\begin{bmatrix} I_a \\ I_b \\ -I_a - I_b \end{bmatrix} \tag{13}$$

The input resistance can be neglected, therefore the input three phase voltage in the stationary ($\alpha\beta$) reference frame can be written as:

$$\begin{bmatrix} U_\alpha \\ U_\beta \end{bmatrix} = L.\begin{bmatrix} \frac{dI_\alpha}{dt} \\ \frac{dI_\beta}{dt} \end{bmatrix} + \begin{bmatrix} V_\alpha \\ V_\beta \end{bmatrix} \tag{14}$$

Consequently, the virtual flux equation is calculated in terms of available input current and converter voltage which eliminates the necessity to use the voltage sensors:

$$\phi_{\alpha\beta} = \int V_{\alpha\beta}dt + LI_{\alpha\beta} \tag{15}$$

In practice, a low-pass filter is used to avoid flux saturating caused by DC offsets in current and voltage sensing. However, this filter changes the flux magnitude and phase. Compensating these errors, a compensator is used which its block diagram has been shown in Figure 3 [13]. The estimated converter flux is as follows:

$$\phi_{conv,\alpha} = \phi'_{conv,\alpha} + \frac{\omega_c}{\omega_e}\phi'_{conv,\beta} \tag{16}$$

$$\phi_{conv,\beta} = \phi'_{conv,\beta} - \frac{\omega_c}{\omega_e}\phi'_{conv,\alpha} \tag{17}$$

where, ω_c is the cutoff frequency of low pass filter in radians per second and ω_e is the synchronous angular frequency which is equal to the fundamental frequency. Equation (18) determines the flux angle.

$$\theta = \tan^{-1}(\frac{\phi_\alpha}{\phi_\beta}) \tag{18}$$

The input instantaneous active and reactive power in stationary αβ coordinate are then given by Equations (19) and (20):

$$P = \frac{3}{2}\omega(\phi_\alpha I_\beta - \phi_\beta I_\alpha) \tag{19}$$

$$Q = \frac{3}{2}\omega(\phi_\alpha I_\alpha + \phi_\beta I_\beta) \tag{20}$$

3. 2. Realizing VF-DPC for Vienna Rectifier In this method, the estimated instantaneous active and reactive powers are compared with their reference values. Errors then pass through two hysteresis controllers which their outputs are defined as d_p and d_q respectively [12].

$$d_p = \begin{cases} 3 & P_{ref} - P > H_p \\ 2 & -H_p \le P_{ref} - P \le H_p \\ 1 & P_{ref} - P < -H_p \end{cases} \tag{21}$$

$$d_q = \begin{cases} 2 & Q_{ref} - Q > H_q \\ 1 & Q_{ref} - Q < -H_q \end{cases} \tag{22}$$

H_p and $H_q$are the hysteresis bands of the active and reactive power controllers. The values assigned to d_p and d_q are based on the comparison between errors and hysteresis band limit. According to Equations (21) and (22), $d_p=3$ and $d_q=2$ show that the active and reactive powers should be increased and as for $d_p=1$ and $d_q=1$ indicate that reduction in both is required.

Due to the three-level nature of the Vienna configuration, balancing the output capacitors voltages is inevitable. This is done by assigning $dp=2$ when the error of active power is between the hysteresis bands. In this case, the control strategy is allocated to capacitors voltage balancing.

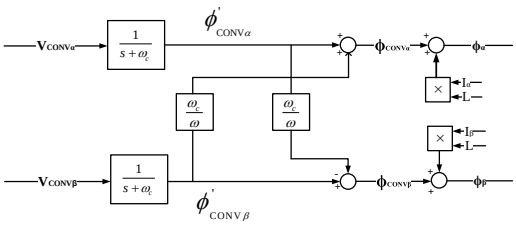

Figure 3. Block diagram of low pass filter and compensator

The hysteresis controller outputs (d_p and d_q) along with the flux sector number and also the value of Δs are then entered in a switching table. Based on the entered values, the proper voltage vector will be applied to Vienna converter. In order to investigate the instantaneous active and reactive power variations in VF-DPC methods, their derivatives are used which are expressed as below [14]:

$$\frac{dP}{dt}=\frac{3}{2}\omega(-(\omega\phi_\alpha I_\alpha+\omega\phi_\beta I_\beta)+\frac{1}{L}(\omega(\phi_\alpha{}^2)+\omega(\phi_\beta{}^2)-\phi_\alpha V_\beta+\phi_\beta V_\alpha)) \quad (23)$$

$$\frac{dQ}{dt}=\frac{3}{2}\omega((\omega\phi_\alpha I_\beta-\omega\phi_\beta I_\alpha)+\phi_\alpha\frac{1}{L}(-\omega\phi_\beta-V_\alpha)+\phi_\beta\frac{1}{L}(-\omega\phi_\alpha-V_\beta)) \quad (24)$$

According to these equations, *dp/dt* and *dq/dt* are dependent on the virtual flux, converter voltage and input current.

3. 3. Vienna Rectifier Space Vectors The Vienna rectifier has 25 voltage space vectors (Figure 4) which are distributed into 6 sectors [15]. Based on the Vienna Rectifier configuration, the voltage and current phase difference varies between -30° and 30°. As the flux lags the voltage by 90°, current is 60° to 120° ahead of flux. Each sector covers 60 degrees which makes the difference between flux and current sector number (Δs) 1 or 2.

For instance, if the flux is in sector 1 and Δs=1, current will be in sector 2 and the allowed switching vectors will be: 1, 2, 3, 12, 13, 14, 24 and 25. However, when Δs=2, current will be in sector 3 and the allowed switching vectors will be: 1, 3, 4, 5, 14, 15, 16 and 25. The impact of Vienna vectors on instantaneous active and reactive power when the flux sector is 1 has been shown in Table 1.

For each sector, the corresponding switching vectors have been listed in Table 2. For example, if dp=1, dq=1 (both instantaneous active and reactive powers have to be reduced) and the flux is in sector 1, vectors V24 and V14 will be applied for Δs=1 and Δs=2, respectively.

Table 3 shows the effect of Vienna space vectors on capacitors voltage balancing. For example, applying V1 will increase Vc1 while decreasing Vc2, so the parameter Δv which is defined as Vc1−Vc2 will be greater than zero. On the other hand, applying V2 will result in Δv< 0.

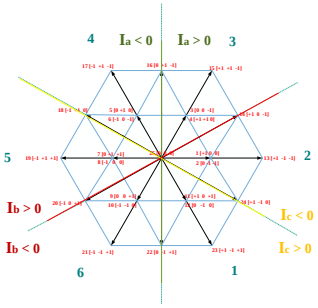

Figure 4. Vienna rectifier space vectors. *(−1, 0,* and *1* denote the connections of phase leg to $-V_{dc}/2$, zero and $V_{dc}/2$, respectively)

TABLE 1. Effect of space vectors on instantaneous active and reactive powers (flux sector is *1*, *Δs* is either *1* or *2*.)

(a)

Δs = 1	Vectors							
	V_1	V_2	V_3	V_{12}	V_{13}	V_{14}	V_{24}	V_{25}
p	↓	↓	↑↑	↑↑	↓	↓	↓↓	↑
q	↓	-	↑↑	↓↓	↓	↑	↓↓	-

(b)

Δs = 2	Vectors							
	V_1	V_3	V_4	V_5	V_{14}	V_{15}	V_{16}	V_{25}
p	↑	↓	↓	↑	↓	↓	↓↓	↑
q	↓	↑	↑↑	↑	↓	↑		-

TABLE 2. Proposed switching table for active and reactive power control

(a)

Δs=1		Flux Sector					
d_p	d_q	1	2	3	4	5	6
1	1	V_{24}	V_{14}	V_{16}	V_{18}	V_{20}	V_{22}
1	2	V_{14}	V_{16}	V_{18}	V_{20}	V_{22}	V_{24}
3	1	V_{12}	V_1	V_4	V_5	V_8	V_9
3	2	V_3	V_5	V_8	V_9	V_{12}	V_1

(b)

Δs=2		Flux Sector					
d_p	d_q	1	2	3	4	5	6
1	1	V_{14}	V_{16}	V_{18}	V_{20}	V_{22}	V_{24}
1	2	V_3	V_{15}	V_{20}	V_9	V_{11}	V_1
3	1	V_1	V_3	V_5	V_8	V_9	V_{12}
3	2	V_5	V_8	V_9	V_{12}	V_1	V_3

The highlighted sections in Table 3 indicate the current sector numbers. As another example, applying V14 to

the Vienna switches will increase Vc1 and Vc2 simultaneously. However, depending on the current sector number (2 or 3), the intensity of voltage increase may be different for capacitors. If the current is in sector 2, C1 will be charged more sharply than C2 and if it is in sector 3, C2 will be charged more sharply than C1.

Figure 5 shows the control block diagram of capacitors voltages. As was mentioned before, with dp= 2 and dq = 1 or 2, the VF-DPC controller act will be based on the reactive power regulation and capacitors voltage balancing.

TABLE 3. Effect of vectors on capacitors voltages (The highlighted sectors indicate the current sector)

Vector No.		V_{c1}	V_{c2}	$\Delta v=v_1-v_2$
1		↑	−	>0
2		−	↑	<0
3		↑	−	>0
4		−	↑	<0
5		↑	−	>0
6		−	↑	<0
7		↑	−	>0
8		−	↑	<0
9		↑	−	>0
10		−	↑	<0
11		↑	−	>0
12		−	↑	<0
13		↑	↑	≈0
14	2	↑↑	↑	>0
	3	↑	↑↑	<0
15		↑	↑	≈0
16	3	↑	↑↑	<0
	4	↑↑	↑	>0
17		↑	↑	≈0
18	4	↑↑	↑	>0
	5	↑	↑↑	<0
19		↑	↑	≈0
20	5	↑	↑↑	<0
	6	↑↑	↑	>0
21		↑	↑	≈0
22	7	↑↑	↑	>0
	1	↑	↑↑	<0
23		↑	↑	≈0
24	1	↑	↑↑	<0
	2	↑↑	↑	>0
25		−	−	≈0

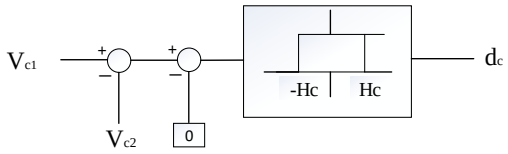

Figure 5. Block diagram of capacitors voltages control

The objective of this control is to minimize Δv. So, it is compared with zero and the error passes through the hysteresis controller. The output of the hysteresis controller is defined as d_c and has been expressed as:

$$d_c = \begin{cases} 2 & \Delta V_{ref} - \Delta V > H_c \\ 1 & \Delta V_{ref} - \Delta V < -H_c \end{cases} \quad (25)$$

where, H_c is the hysteresis band. Table 4 shows the proposed switching table based on the reactive power regulation and capacitors voltage balancing.

Figure 6 shows the complete control block diagram of the proposed virtual flux based direct power control (VF-DPC) for Vienna rectifier.

Firstly, the output voltage is compared with the reference voltage (V_{dc}, *ref*) producing an error signal. This signal is then passed through a proportional-integral (PI) controller and the output value is multiplied by V_{dc} to generate P_{ref}. The comparison of P_{ref} with the estimated active power (P_{est}) leads to an error which in turn enters the hysteresis band controller. At the same time, in order to achieve the unity power factor at the grid side, the estimated reactive power (Q_{est}) should be compared to its reference zero value. Result of this comparison enters another hysteresis band controller. As was mentioned before, the hysteresis controllers' outputs are defined as d_p and d_q. d_p, d_q and Δv are the switching table inputs which determine the proper switching states for the Vienna rectifier.

The P_{est} and Q_{est} values are calculated in the instantaneous active and reactive power estimation block using Equations (19) and (20). I_α, I_β, ϕ_α and ϕ_β are the entries to this section which are computed in the virtual flux estimator block regarding Equations (8)-(15) independent of sensing the three phase grid voltage.

4. SIMULATION RESULTS

In order to verify the VF-DPC performance on Vienna rectifier, software implementation of Figure 6 has been carried out with MATLAB/Simulink. Table 5 shows the simulation parameters. The proportional and integral gains of the PI controller are set to 0.1 and 1, respectively and are obtained by trial and error.

Figure 7 shows the three-phase input line current. As can be seen from the figure, although the current regulation loop has been omitted in the VF-DPC control technique, it has the ability of controlling the current in

sinusoidal waveform. The input current THD is 2.65% which is under the permitted limit imposed by IEEE std. 519-1992.

Figure 8 shows both the voltage and current of phase "a" at unity power factor. Getting the unity input power factor, reference value of the reactive power should be set to zero.

TABLE 4. Proposed switching table for capacitors voltages and reactive power control

(a)

Δs=1		Flux Sector					
d_c	d_q	1	2	3	4	5	6
1	1	V_{12}	V_{14}	V_4	V_{18}	V_8	V_{22}
1	2	V_4	V_{16}	V_8	V_{20}	V_{12}	V_{24}
2	1	V_{24}	V_1	V_{16}	V_5	V_{20}	V_9
2	2	V_{14}	V_5	V_{18}	V_9	V_{22}	V_1

(b)

Δs=2		Flux Sector					
d_c	d_q	1	2	3	4	5	6
1	1	V_{14}	V_4	V_{18}	V_8	V_{22}	V_{12}
1	2	V_4	V_6	V_{20}	V_{12}	V_{24}	V_4
2	1	V_1	V_3	V_5	V_{20}	V_9	V_{24}
2	2	V_5	V_{18}	V_7	V_{22}	V_1	V_1

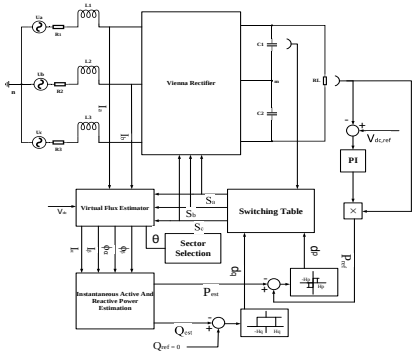

Figure 6. Block Diagram of VF-DPC

TABLE 5. Simulation parameters

Input phase voltage	50 V (RMS)
Fundamental frequency	50 Hz
Cutoff frequency (ω_c)	100π rad/sec
Input power supply inductance	15 mH
Output DC voltage	200 V
Load resistance	100 Ω
DC-link Capacitors C_1,C_2	2.2 mF

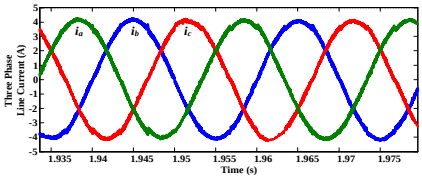

Figure 7. Input three phase line current

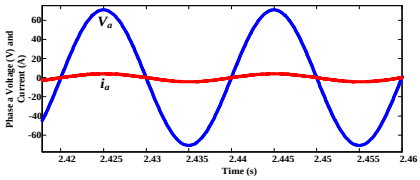

Figure 8. Phase "a" voltage and current at unity power factor

Figures 9 (a) and (b) show the DC link voltage and capacitors voltages respectively which accurately track their references values.

Figure 10 shows the output voltage transient responses to the step changes in the DC voltage reference. Changes are from *200V* to *250V* at $t = 1$ sec and from *250V* to *200V* at $t = 2$ sec. As can be seen, the output voltage follows its references with acceptable transient due to the fine tuning of the PI controller.

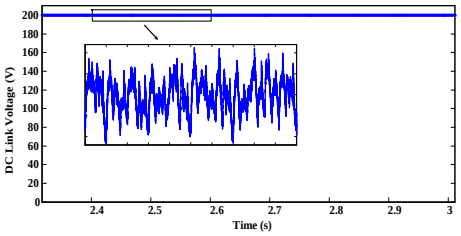

(a)

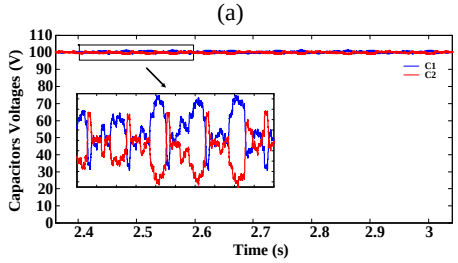

(b)

Figure 9. (a) DC link voltage (b) Capacitors voltages

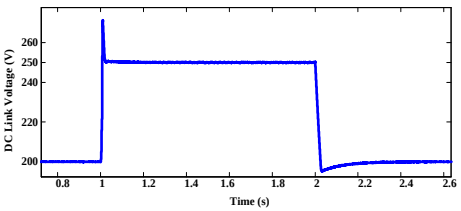

Figure 10. Transient response for the step changes of dc-link voltage

Figure 11 shows the output voltage, active and reactive powers and also the input phase voltage and current at the presence of a load changing. The output load resistance has been decreased to *50 Ω* at *t = 2* sec.

As is depicted in Figure 11, the output voltage tracks its reference with a 6% undershoot and a settling time about 0.07 sec (3.5 cycles). Moreover, the active power has been increased due to the load rise while the reactive power remains zero. It means that the power estimation section estimates the instantaneous active and reactive powers separately, accurately and independent of any input voltage sensors. Also, the input phase voltage and current still stay in-phase. These are due to the satisfactory performance of the proposed VF-DPC controller for the Vienna rectifier.

In order to compare the proposed VF-DPC method with conventional techniques, some simulations have been carried out for a CB-PWM strategy [16]. Simulation parameters are the same as Table 5 except for the cutoff frequency that is not used in conventional CB-PWM techniques. Figure 12 shows the input three phase line current which is sinusoidal and has a satisfactory THD (1.37%). This is because of the internal current control loop used in conventional methods [16].

Figures 13 (a) and (b) show the DC link voltage and capacitors voltages respectively in the conventional method which accurately track their references values.

The comparison between two proposed and conventional methods proves the efficiency of applying VF-DPC on the Vienna rectifier. It satisfies the input current THD limit and also is capable of achieving the unity power factor. The controllability of the output voltage along with the capacitors voltages balancing also has been proved. Moreover, it has less number of sensors and better dynamic performance due to its hysteresis band controllers.

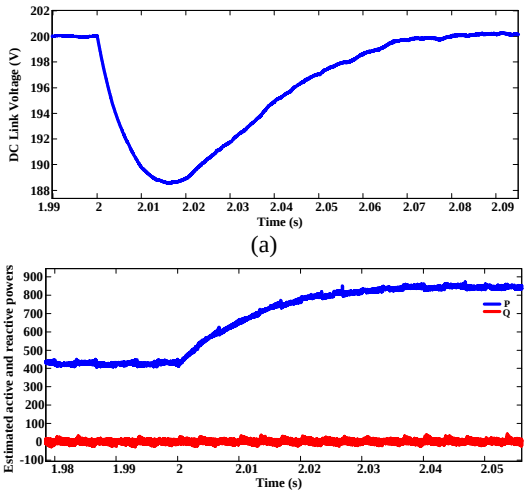

(a)

(b)

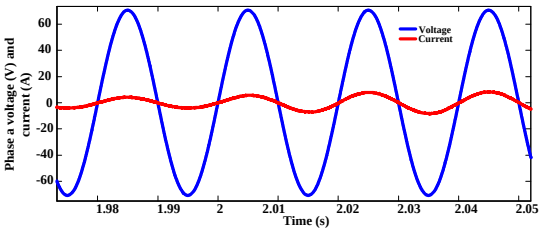

(c)

Figure 11. Transient response for load variation from low to high current demand for the VF-DPC with new switching table, a) DC-link voltage, b) Estimated active and reactive powers and c) Phase a current and voltage

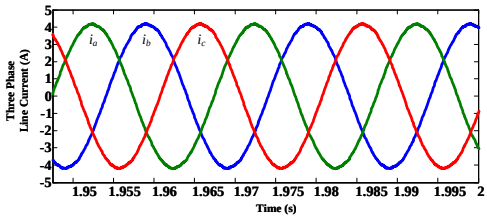

Figure 12. Input three phase line current in CB-PWM method

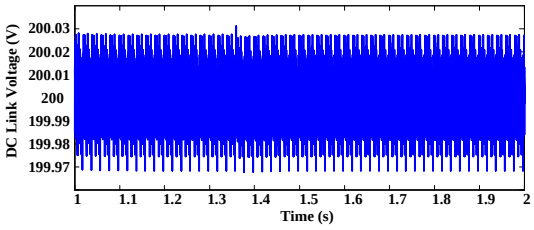

(a)

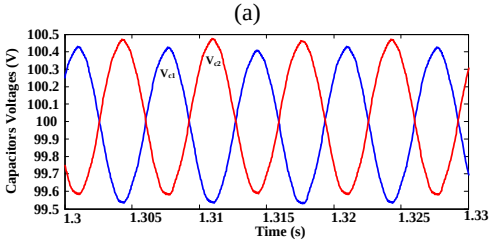

(b)

Figure 13. (a) DC link voltage (b) Capacitors voltages

5. CONCLUSION

In this paper, the VF-DPC method which has been applied to the conventional two-level PWM rectifiers, has been proposed for the Vienna rectifier. However, due to the three-level nature of the Vienna configuration, balancing the output capacitors voltages is of considerable importance. This has led to an adapted switching table for the proposed virtual flux based technique. Applying this reform, simulation results have shown the high performance of the proposed VF-DPC for the Vienna rectifier.

6. REFERENCES

1. Hosseini, S. and Mohammadi, H., "Neural network implementation of a three phase regulated pwm ac to dc converter with input unbalance correction", ***International Journal of Engineering***, Vol. 9, No. 3, (1996), 151-158.
2. Savio, M. and Murugesan, S., "Space vector control scheme of three level zsi applied to wind energy systems", ***International Journal of Engineering-Transactions C: Aspects***, Vol. 25, No. 4, (2012), 275.
3. Kolar, J.W. and Friedli, T., "The essence of three-phase pfc rectifier systems—part i", ***IEEE Transactions on Power Electronics***, Vol. 28, No. 1, (2013), 176-198.
4. Carlton, D. and Dunford, W.G., "Multi-level, uni-directional ac-dc converters, a cost effective alternative to bi-directional converters", in Power Electronics Specialists Conference, 2001. PESC. 2001 IEEE 32nd Annual, IEEE. Vol. 4, (2001), 1911-1916.
5. Teichmann, R., Malinowski, M. and Bernet, S., "Evaluation of three-level rectifiers for low-voltage utility applications", ***IEEE Transactions on Industrial Electronics***, Vol. 52, No. 2, (2005), 471-481.
6. Jiang, X., Yang, J., Han, J. and Tang, T., "A survey of cascaded multi-level pwm rectifier with vienna modules for hvdc system", in Power Electronics and Application Conference and Exposition (PEAC), 2014 International, IEEE. (2014), 72-77.
7. Dalessandro, L., Round, S.D., Drofenik, U. and Kolar, J.W., "Discontinuous space-vector modulation for three-level pwm rectifiers", ***IEEE Transactions on Power Electronics***, Vol. 23, No. 2, (2008), 530-542.
8. Jiang, W.-d., Du, S.-w., Chang, L.-c., Zhang, Y. and Zhao, Q., "Hybrid pwm strategy of svpwm and vsvpwm for npc three-level voltage-source inverter", ***IEEE Transactions on Power Electronics***, Vol. 25, No. 10, (2010), 2607-2619.
9. Ogasawara, S. and Akagi, H., "Analysis of variation of neutral point potential in neutral-point-clamped voltage source pwm inverters", in Industry Applications Society Annual Meeting, 1993., Conference Record of the 1993 IEEE, (1993), 965-970.
10. Pou, J., Boroyevich, D. and Pindado, R., "Effects of imbalances and nonlinear loads on the voltage balance of a neutral-point-clamped inverter", ***IEEE Transactions on Power Electronics***, Vol. 20, No. 1, (2005), 123-131.
11. He, L. and Chen, X., "A neutral point potential balance control strategy based on vector controlled vienna rectifier", in Energy Conversion Congress and Exposition (ECCE), 2010 IEEE, (2010), 2060-2065.
12. Malinowski, M., Kazmierkowski, M.P., Hansen, S., Blaabjerg, F. and Marques, G., "Virtual-flux-based direct power control of three-phase pwm rectifiers", ***IEEE Transactions on Industry Applications***, Vol. 37, No. 4, (2001), 1019-1027.
13. Idris, N.R.N. and Yatim, A.H.M., "An improved stator flux estimation in steady-state operation for direct torque control of induction machines", ***IEEE Transactions on Industry Applications***, Vol. 38, No. 1, (2002), 110-116.
14. Espinoza, J.E., Espinoza, J.R. and Morán, L.A., "A systematic controller-design approach for neutral-point-clamped three-level inverters", ***IEEE Transactions on Industrial Electronics***, Vol. 52, No. 6, (2005), 1589-1599.
15. Celanovic, N. and Boroyevich, D., "A comprehensive study of neutral-point voltage balancing problem in three-level neutral-point-clamped voltage source pwm inverters", ***IEEE Transactions on Power Electronics***, Vol. 15, No. 2, (2000), 242-249.
16. Hang, L., Li, B., Zhang, M., Wang, Y. and Tolbert, L.M., "Equivalence of svm and carrier-based pwm in three-phase/wire/level vienna rectifier and capability of unbalanced-load control", ***IEEE Transactions on Industrial Electronics***, Vol. 61, No. 1, (2014), 20-28.

Virtual Flux Based Direct Power Control on Vienna Rectifier

M. Rasouli Khatir, H. Ghoreishy, S. A. Gholamian

Electrical and Computer Engineering, Babol Noushirvany University of Technology, Babol, Iran

P A P E R I N F O

Paper history:
Received 13 October 2017
Received in revised form 10 November 2017
Accepted 02 December 2017

Keywords:
Capacitor Voltage Balancing
Direct Power Control
Vienna Rectifier
Virtual Flux

چکیده

در این مقاله، کنترل مستقیم توان بر مبنای شار مجازی برای یکسوساز وی‌ینا پیشنهاد گردیده است. عدم نیاز به سنسورهای ولتاژ ورودی، عدم نیاز به حلقه تنظیم جریان و بلوک مدولاسیون پهنای پالس ولتاژ به همراه مجزا سازی توانهای اکتیو و راکتیو، برخی از مزایای برجسته این روش هستند که آن را برای کنترل یکسوسازهای اکتیو متعارف مناسب ساخته‌اند. با این حال، به دلیل ماهیت سه سطحی ساختار وی‌ینا، متعادل سازی ولتاژ خازنهای خروجی امری اجتناب ناپذیر است و منجر به پیشنهاد تکنیک تغییر یافته‌ای بر مبنای شار مجازی در این مقاله گشته است. با اعمال تغییرات مذکور، یک جدول کلیدزنی مجزا جهت کنترل ولتاژ خازنها در داخل تکنیک مذکور گنجانده شده است. نتایج شبیه سازی برتری روش پیشنهادی شار مجازی را از نقطه نظر مزایای ذکر شده نسبت به سایر تکنیکهای کنترلی وی‌ینا نشان می‌دهد.

***doi**: 10.5829/ije.2018.31.02b.12*